

Curing the high-energy perturbative instability of quarkonium (photo)production cross sections

J.P. Lansberg

IJCLab Orsay – Paris-Saclay U. – CNRS

Quarkonium Working Group 2024

26/02/24 - 01/03/24 – IISER Mohali, India

Work done in collaboration with M. Nefedov, M.A. Ozcelik
& A. Colpani Serri, Y. Feng, C. Flore, H.S. Shao, Y. Yedelkina



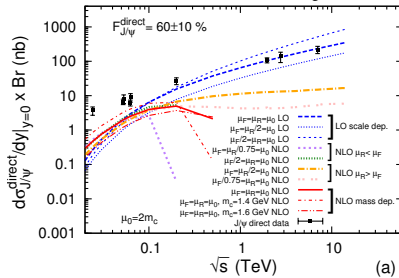
This project is supported by the European Union's Horizon 2020 research and innovation programme under Grant agreement no. 824093



Negative quarkonium P_T -integrated cross sections at NLO

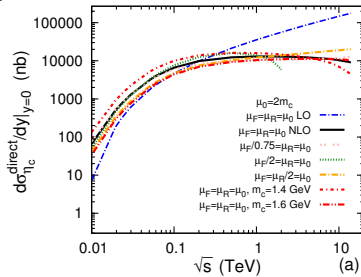
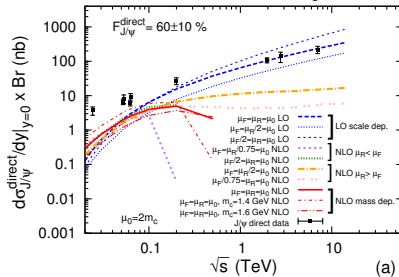
Negative quarkonium P_T -integrated cross sections at NLO

[Y. Feng, JPL, J.X. Wang, EPJC 75 (2015) 313]



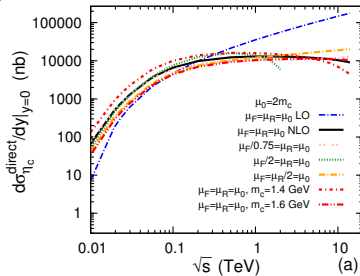
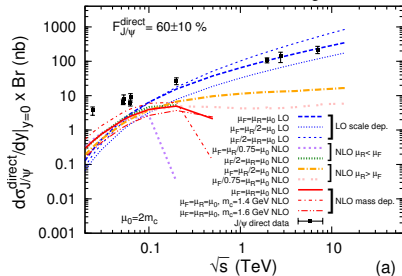
Negative quarkonium P_T -integrated cross sections at NLO

[Y. Feng, JPL, J.X. Wang, EPJC 75 (2015) 313]

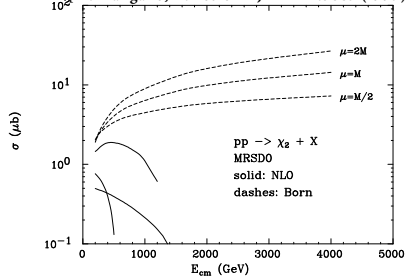


Negative quarkonium P_T -integrated cross sections at NLO

[Y. Feng, JPL, J.X. Wang, EPJC 75 (2015) 313]

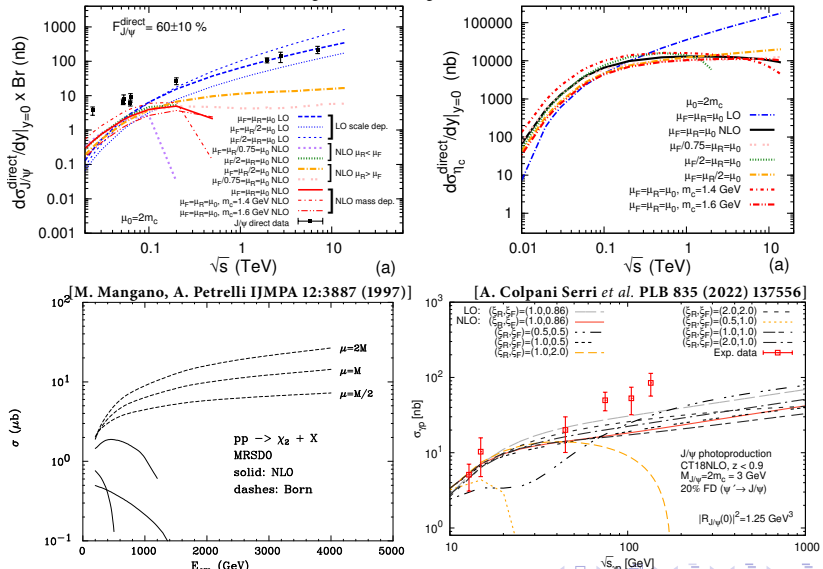


[M. Mangano, A. Petrelli IJMPA 12:3887 (1997)]



Negative quarkonium P_T -integrated cross sections at NLO

[Y. Feng, JPL, J.X. Wang, EPJC 75 (2015) 313]



Historical developments

Historical developments

- In 1992, J. Kühn & E. Mirkes compute $\sigma(pp \rightarrow \eta_t X)$ at NLO [J. Kühn, E. Mirkes, PLB 296 (1992) 425]

Historical developments

- In 1992, J. Kühn & E. Mirkes compute $\sigma(pp \rightarrow \eta_t X)$ at NLO [J. Kühn, E. Mirkes, PLB 296 (1992) 425]
- In 1994, G. Schuler's review in 1994
 - confirms results by J. Kühn & E. Mirkes
 - points out at issues with negative cross sections at high energies
 - explains why, for some gluon PDFs, appearance of strong/weak μ_F dependence

Historical developments

- In 1992, J. Kühn & E. Mirkes compute $\sigma(pp \rightarrow \eta tX)$ at NLO [J. Kühn, E. Mirkes, PLB 296 (1992) 425]
- In 1994, G. Schuler's review in 1994
 - confirms results by J. Kühn & E. Mirkes
 - points out at issues with negative cross sections at high energies
 - explains why, for some gluon PDFs, appearance of strong/weak μ_F dependence
- In 1996, M. Mangano reaches same conclusions [M.L. Mangano, A. Petrelli, IJMPA 12 (1997) 3887]

[¶]Most of the remarks which follow have already been made by G. Schuler in his '94 review [9]. Schuler at the time had available the full NLO corrections to η production, as well as the leading small- x behaviour of the χ cross sections. It is a pity that those remarks have passed almost unnoticed in the community!

- Desastrous results for χ_{c2} (previous slide)

Historical developments

- In 1992, J. Kühn & E. Mirkes compute $\sigma(pp \rightarrow \eta tX)$ at NLO [J. Kühn, E. Mirkes, PLB 296 (1992) 425]
- In 1994, G. Schuler's review in 1994
 - confirms results by J. Kühn & E. Mirkes
 - points out at issues with negative cross sections at high energies
 - explains why, for some gluon PDFs, appearance of strong/weak μ_F dependence
- In 1996, M. Mangano reaches same conclusions [M.L. Mangano, A. Petrelli, IJMPA 12 (1997) 3887]

[†]Most of the remarks which follow have already been made by G. Schuler in his '94 review [9]. Schuler at the time had available the full NLO corrections to η production, as well as the leading small- x behaviour of the χ cross sections. It is a pity that those remarks have passed almost unnoticed in the community!

- Desastrous results for χ_{c2} (previous slide)
- In 1998, A. Petrelli *et al.* get full NRQCD NLO results [A. Petrelli et al., NPB 514 (1998) 245-309]
 - First results for $^1S_0^{[8]}$, $^3P_J^{[8]}$, $^3S_1^{[8]}$
 - Only pheno attempt in 2006 ... at low energies [F. Maltoni & Hera-b PLB 638 (2006) 202]

Historical developments

- In 1992, J. Kühn & E. Mirkes compute $\sigma(pp \rightarrow \eta tX)$ at NLO [J. Kühn, E. Mirkes, PLB 296 (1992) 425]
- In 1994, G. Schuler's review in 1994
 - confirms results by J. Kühn & E. Mirkes
 - points out at issues with negative cross sections at high energies
 - explains why, for some gluon PDFs, appearance of strong/weak μ_F dependence
- In 1996, M. Mangano reaches same conclusions [M.L. Mangano, A. Petrelli, IJMPA 12 (1997) 3887]

[†]Most of the remarks which follow have already been made by G. Schuler in his '94 review [9]. Schuler at the time had available the full NLO corrections to η production, as well as the leading small- x behaviour of the χ cross sections. It is a pity that those remarks have passed almost unnoticed in the community!

- Desastrous results for χ_{c2} (previous slide)
- In 1998, A. Petrelli *et al.* get full NRQCD NLO results [A. Petrelli et al., NPB 514 (1998) 245-309]
 - First results for $^1S_0^{[8]}, ^3P_J^{[8]}, ^3S_1^{[8]}$
 - Only pheno attempt in 2006 ... at low energies [F. Maltoni & Hera-b PLB 638 (2006) 202]
- Much later, we reached the same conclusions [M.A. Ozcelik, PoS DIS2019 (2019) 159, Y. Feng, JPL, J.X. Wang, Eur.Phys.J. C75 (2015) 313]

Historical developments

- In 1992, J. Kühn & E. Mirkes compute $\sigma(pp \rightarrow \eta tX)$ at NLO [J. Kühn, E. Mirkes, PLB 296 (1992) 425]
- In 1994, G. Schuler's review in 1994
 - confirms results by J. Kühn & E. Mirkes
 - points out at issues with negative cross sections at high energies
 - explains why, for some gluon PDFs, appearance of strong/weak μ_F dependence
- In 1996, M. Mangano reaches same conclusions [M.L. Mangano, A. Petrelli, IJMPA 12 (1997) 3887]

[†]Most of the remarks which follow have already been made by G. Schuler in his '94 review [9]. Schuler at the time had available the full NLO corrections to η production, as well as the leading small- x behaviour of the χ cross sections. It is a pity that those remarks have passed almost unnoticed in the community!

- Desastrous results for χ_{c2} (previous slide)
- In 1998, A. Petrelli *et al.* get full NRQCD NLO results [A. Petrelli et al., NPB 514 (1998) 245-309]
 - First results for $^1S_0^{[8]}, ^3P_J^{[8]}, ^3S_1^{[8]}$
 - Only pheno attempt in 2006 ... at low energies [F. Maltoni & Hera-b PLB 638 (2006) 202]
- Much later, we reached the same conclusions [M.A. Ozcelik, PoS DIS2019 (2019) 159, Y. Feng, JPL, J.X. Wang, Eur.Phys.J. C75 (2015) 313]
- and, by digging out, same problem in $\gamma p \rightarrow \psi X$ found [A. Colpani Serri et al. PLB 835 (2022) 137556]

The NLO partonic cross section at large \hat{s}

The **partonic high-energy limit** is defined as taking $\hat{\sigma}$ at $\hat{s} \rightarrow \infty$ or equivalently $z \rightarrow 0$ with $z = \frac{M_Q^2}{\hat{s}}$,

$$\lim_{z \rightarrow 0} \hat{\sigma}_{gg}^{\text{NLO}}(z) = 2C_A \frac{\alpha_s}{\pi} \hat{\sigma}_0^{\text{LO}} \left(\log \frac{M_Q^2}{\mu_F^2} + A_{gg} \right) \quad (1)$$

$$\lim_{z \rightarrow 0} \hat{\sigma}_{qg}^{\text{NLO}}(z) = C_F \frac{\alpha_s}{\pi} \hat{\sigma}_0^{\text{LO}} \left(\log \frac{M_Q^2}{\mu_F^2} + A_{qg} \right) \quad (2)$$

The NLO partonic cross section at large \hat{s}

The **partonic high-energy limit** is defined as taking $\hat{\sigma}$ at $\hat{s} \rightarrow \infty$ or equivalently $z \rightarrow 0$ with $z = \frac{M_Q^2}{\hat{s}}$,

$$\lim_{z \rightarrow 0} \hat{\sigma}_{gg}^{\text{NLO}}(z) = 2C_A \frac{\alpha_s}{\pi} \hat{\sigma}_0^{\text{LO}} \left(\log \frac{M_Q^2}{\mu_F^2} + A_{gg} \right) \quad (1)$$

$$\lim_{z \rightarrow 0} \hat{\sigma}_{qg}^{\text{NLO}}(z) = C_F \frac{\alpha_s}{\pi} \hat{\sigma}_0^{\text{LO}} \left(\log \frac{M_Q^2}{\mu_F^2} + A_{qg} \right) \quad (2)$$

- for ${}^1S_0^{[1,8]}$:

$$A_{gg} = A_{qg} = -1$$

The NLO partonic cross section at large \hat{s}

The **partonic high-energy limit** is defined as taking $\hat{\sigma}$ at $\hat{s} \rightarrow \infty$ or equivalently $z \rightarrow 0$ with $z = \frac{M_Q^2}{\hat{s}}$,

$$\lim_{z \rightarrow 0} \hat{\sigma}_{gg}^{\text{NLO}}(z) = 2C_A \frac{\alpha_s}{\pi} \hat{\sigma}_0^{\text{LO}} \left(\log \frac{M_Q^2}{\mu_F^2} + A_{gg} \right) \quad (1)$$

$$\lim_{z \rightarrow 0} \hat{\sigma}_{qg}^{\text{NLO}}(z) = C_F \frac{\alpha_s}{\pi} \hat{\sigma}_0^{\text{LO}} \left(\log \frac{M_Q^2}{\mu_F^2} + A_{qg} \right) \quad (2)$$

- for ${}^1S_0^{[1,8]}$: $A_{gg} = A_{qg} = -1$
- for $\mu_F = M_Q$, $\hat{\sigma}_{ig}^{\text{NLO}}(\hat{s} \rightarrow \infty) \propto -\frac{\alpha_s}{\pi} \hat{\sigma}_0^{\text{LO}}$

The NLO partonic cross section at large \hat{s}

The **partonic high-energy limit** is defined as taking $\hat{\sigma}$ at $\hat{s} \rightarrow \infty$ or equivalently $z \rightarrow 0$ with $z = \frac{M_Q^2}{\hat{s}}$,

$$\lim_{z \rightarrow 0} \hat{\sigma}_{gg}^{\text{NLO}}(z) = 2C_A \frac{\alpha_s}{\pi} \hat{\sigma}_0^{\text{LO}} \left(\log \frac{M_Q^2}{\mu_F^2} + A_{gg} \right) \quad (1)$$

$$\lim_{z \rightarrow 0} \hat{\sigma}_{qg}^{\text{NLO}}(z) = C_F \frac{\alpha_s}{\pi} \hat{\sigma}_0^{\text{LO}} \left(\log \frac{M_Q^2}{\mu_F^2} + A_{qg} \right) \quad (2)$$

- for ${}^1S_0^{[1,8]}$: $A_{gg} = A_{qg} = -1$
- for $\mu_F = M_Q$, $\hat{\sigma}_{ig}^{\text{NLO}}(\hat{s} \rightarrow \infty) \propto -\frac{\alpha_s}{\pi} \hat{\sigma}_0^{\text{LO}}$
- this limit contributes most for “flat” gluon PDFs at low x

The NLO partonic cross section at large \hat{s}

The **partonic high-energy limit** is defined as taking $\hat{\sigma}$ at $\hat{s} \rightarrow \infty$ or equivalently $z \rightarrow 0$ with $z = \frac{M_Q^2}{\hat{s}}$,

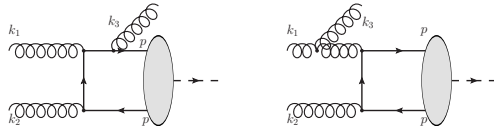
$$\lim_{z \rightarrow 0} \hat{\sigma}_{gg}^{\text{NLO}}(z) = 2C_A \frac{\alpha_s}{\pi} \hat{\sigma}_0^{\text{LO}} \left(\log \frac{M_Q^2}{\mu_F^2} + A_{gg} \right) \quad (1)$$

$$\lim_{z \rightarrow 0} \hat{\sigma}_{qg}^{\text{NLO}}(z) = C_F \frac{\alpha_s}{\pi} \hat{\sigma}_0^{\text{LO}} \left(\log \frac{M_Q^2}{\mu_F^2} + A_{qg} \right) \quad (2)$$

- for ${}^1S_0^{[1,8]}$: $A_{gg} = A_{qg} = -1$
- for $\mu_F = M_Q$, $\hat{\sigma}_{ig}^{\text{NLO}}(\hat{s} \rightarrow \infty) \propto -\frac{\alpha_s}{\pi} \hat{\sigma}_0^{\text{LO}}$
- this limit contributes most for “flat” gluon PDFs at low x
- If PDFs are not steep (evolved) enough, the large- \hat{s} region dominates and the hadronic cross section becomes negative

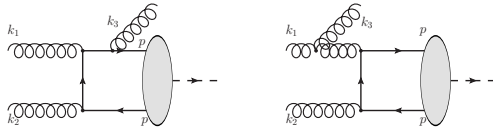
Recap of NLO calculation & origin of negative numbers

\hat{s} -dependence only present in real corrections ($g(k_1) + g(k_2) \rightarrow \eta_Q(P) + g(k_3)$)



Recap of NLO calculation & origin of negative numbers

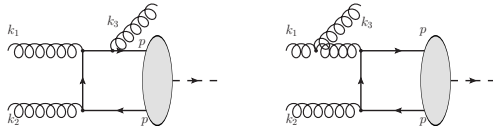
\hat{s} -dependence only present in real corrections ($g(k_1) + g(k_2) \rightarrow \eta_Q(P) + g(k_3)$)



- Real-emission corrections are perfect square ($|\mathcal{M}^{(\text{Real})}|^2$) and thus positive

Recap of NLO calculation & origin of negative numbers

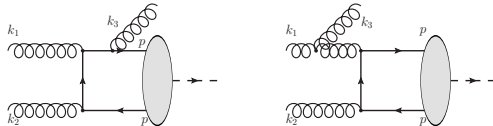
\hat{s} -dependence only present in real corrections ($g(k_1) + g(k_2) \rightarrow \eta_Q(P) + g(k_3)$)



- Real-emission corrections are perfect square ($|\mathcal{M}^{(\text{Real})}|^2$) and thus positive
- IR singularities in the real emissions only reveal themselves after taking the phase-space integration: $\bar{\sigma}_{gg}^{\text{NLO}, z \neq 1}(z) = \int d\hat{t} \frac{\bar{\sigma}_{gg}^{\text{NLO}, z \neq 1}}{d\hat{t}}$

Recap of NLO calculation & origin of negative numbers

\hat{s} -dependence only present in real corrections ($g(k_1) + g(k_2) \rightarrow \eta_Q(P) + g(k_3)$)



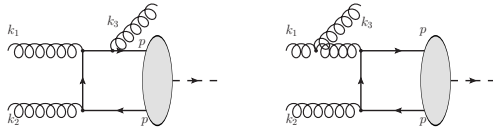
- Real-emission corrections are perfect square ($|\mathcal{M}^{(\text{Real})}|^2$) and thus positive
- IR singularities in the real emissions only reveal themselves after taking the

$$\text{phase-space integration: } \overline{\sigma}_{gg}^{\text{NLO}, z \neq 1}(z) = \int d\hat{t} \frac{\overline{\sigma}_{gg}^{\text{NLO}, z \neq 1}}{d\hat{t}}$$

$$\overline{\sigma}_{gg}^{\text{NLO}, z \neq 1}(z) = -\frac{1}{\epsilon_{\text{IR}}} \frac{\alpha_s}{\pi} \left(\frac{4\pi\mu_R^2}{M_Q^2} \right)^\epsilon \Gamma(1+\epsilon) \hat{\sigma}_0^{\text{LO}} z P_{gg}(z) + 2C_A \frac{\alpha_s}{\pi} \hat{\sigma}_0^{\text{LO}} \overline{A}_{gg}(z)$$

Recap of NLO calculation & origin of negative numbers

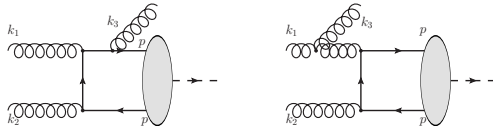
\hat{s} -dependence only present in real corrections ($g(k_1) + g(k_2) \rightarrow \eta_Q(P) + g(k_3)$)



- Real-emission corrections are perfect square ($|\mathcal{M}^{(\text{Real})}|^2$) and thus positive
- IR singularities in the real emissions only reveal themselves after taking the phase-space integration: $\overline{\sigma}_{gg}^{\text{NLO}, z \neq 1}(z) = \int d\hat{t} \frac{\overline{\sigma}_{gg}^{\text{NLO}, z \neq 1}}{d\hat{t}}$
$$\overline{\sigma}_{gg}^{\text{NLO}, z \neq 1}(z) = -\frac{1}{\epsilon_{\text{IR}}} \frac{\alpha_s}{\pi} \left(\frac{4\pi\mu_R^2}{M_Q^2} \right)^\epsilon \Gamma(1+\epsilon) \hat{\sigma}_0^{\text{LO}} z P_{gg}(z) + 2C_A \frac{\alpha_s}{\pi} \hat{\sigma}_0^{\text{LO}} \overline{A}_{gg}(z)$$
- For $\epsilon_{\text{IR}} \rightarrow 0^-$, $\overline{\sigma}_{gg}^{\text{NLO}, z \neq 1} \geq 0$ for all $0 \leq z < 1$ as expected

Recap of NLO calculation & origin of negative numbers

\hat{s} -dependence only present in real corrections ($g(k_1) + g(k_2) \rightarrow \eta_Q(P) + g(k_3)$)



- Real-emission corrections are perfect square ($|\mathcal{M}^{(\text{Real})}|^2$) and thus positive
- IR singularities in the real emissions only reveal themselves after taking the

phase-space integration: $\bar{\sigma}_{gg}^{\text{NLO}, z \neq 1}(z) = \int d\hat{t} \frac{\hat{\sigma}_{gg}^{\text{NLO}, z \neq 1}}{d\hat{t}}$

$$\bar{\sigma}_{gg}^{\text{NLO}, z \neq 1}(z) = -\frac{1}{\epsilon_{\text{IR}}} \frac{\alpha_s}{\pi} \left(\frac{4\pi\mu_R^2}{M_Q^2} \right)^\epsilon \Gamma(1+\epsilon) \hat{\sigma}_0^{\text{LO}} z P_{gg}(z) + 2C_A \frac{\alpha_s}{\pi} \hat{\sigma}_0^{\text{LO}} \bar{A}_{gg}(z)$$

- For $\epsilon_{\text{IR}} \rightarrow 0^-$, $\bar{\sigma}_{gg}^{\text{NLO}, z \neq 1} \geq 0$ for all $0 \leq z < 1$ as expected
- Initial-state collinear divergences are absorbed/subtracted into PDF via process-independent Altarelli-Parisi counterterm in $\overline{\text{MS}}$ -scheme

$$\bar{\sigma}_{gg}^{\text{AP-CT}}(z) = \frac{1}{\epsilon_{\text{IR}}} \frac{\alpha_s}{\pi} \left(\frac{4\pi\mu_R^2}{\mu_F^2} \right)^\epsilon \Gamma(1+\epsilon) \hat{\sigma}_0^{\text{LO}} z P_{gg}(z)$$

A new scale-choice prescription

JPL, M.A. Ozcelik, EPJC 81 (2021) 6, 497

A new scale-choice prescription

JPL, M.A. Ozcelik, EPJC 81 (2021) 6, 497

- The subtraction of the AP CT in the $\overline{\text{MS}}$ -scheme then yields :

$$\lim_{z \rightarrow 0} \hat{\sigma}_{(g,q)g}^{\text{NLO}}(z) = (2C_A, C_F) \frac{\alpha_s}{\pi} \hat{\sigma}_0^{\text{LO}} \left(\log \frac{M_Q^2}{\mu_F^2} + A_{(g,q)g} \right) \quad (3)$$

A new scale-choice prescription

JPL, M.A. Ozcelik, EPJC 81 (2021) 6, 497

- The subtraction of the AP CT in the $\overline{\text{MS}}$ -scheme then yields :

$$\lim_{z \rightarrow 0} \hat{\sigma}_{(g,q)g}^{\text{NLO}}(z) = (2C_A, C_F) \frac{\alpha_s}{\pi} \hat{\sigma}_0^{\text{LO}} \left(\log \frac{M_Q^2}{\mu_F^2} + A_{(g,q)g} \right) \quad (3)$$

- In principle, the subtraction should be compensated by the PDF evolution

A new scale-choice prescription

JPL, M.A. Ozcelik, EPJC 81 (2021) 6, 497

- The subtraction of the AP CT in the $\overline{\text{MS}}$ -scheme then yields :

$$\lim_{z \rightarrow 0} \hat{\sigma}_{(g,q)g}^{\text{NLO}}(z) = (2C_A, C_F) \frac{\alpha_s}{\pi} \hat{\sigma}_0^{\text{LO}} \left(\log \frac{M_Q^2}{\mu_F^2} + A_{(g,q)g} \right) \quad (3)$$

- In principle, the subtraction should be compensated by the PDF evolution
- PDF evolution is universal, not $A_{ij} \rightarrow \hat{\sigma} < 0$ can arise from this subtraction

A new scale-choice prescription

JPL, M.A. Ozcelik, EPJC 81 (2021) 6, 497

- The subtraction of the AP CT in the $\overline{\text{MS}}$ -scheme then yields :

$$\lim_{z \rightarrow 0} \hat{\sigma}_{(g,q)g}^{\text{NLO}}(z) = (2C_A, C_F) \frac{\alpha_s}{\pi} \hat{\sigma}_0^{\text{LO}} \left(\log \frac{M_Q^2}{\mu_F^2} + A_{(g,q)g} \right) \quad (3)$$

- In principle, the subtraction should be compensated by the PDF evolution
- PDF evolution is universal, not $A_{ij} \rightarrow \hat{\sigma} < 0$ can arise from this subtraction
- $A_{gg} = A_{qg}$ allows us to propose a new scale prescription for μ_F ,

$$\mu_F = \hat{\mu}_F \equiv M_Q e^{A_{gg,qg}/2} \text{ such that } \left(\log \frac{M_Q^2}{\mu_F^2} + A_{gg,qg} \right) = 0 \text{ and } \lim_{z \rightarrow 0} \hat{\sigma}_{gg,qg}^{\text{NLO}}(z) = 0$$

A new scale-choice prescription

JPL, M.A. Ozcelik, EPJC 81 (2021) 6, 497

- The subtraction of the AP CT in the $\overline{\text{MS}}$ -scheme then yields :

$$\lim_{z \rightarrow 0} \hat{\sigma}_{(g,q)g}^{\text{NLO}}(z) = (2C_A, C_F) \frac{\alpha_s}{\pi} \hat{\sigma}_0^{\text{LO}} \left(\log \frac{M_Q^2}{\mu_F^2} + A_{(g,q)g} \right) \quad (3)$$

- In principle, the subtraction should be compensated by the PDF evolution
- PDF evolution is universal, not $A_{ij} \rightarrow \hat{\sigma} < 0$ can arise from this subtraction
- $A_{gg} = A_{qg}$ allows us to propose a new scale prescription for μ_F ,

$$\mu_F = \hat{\mu}_F \equiv M_Q e^{A_{gg,qg}/2} \quad \text{such that } \left(\log \frac{M_Q^2}{\mu_F^2} + A_{gg,qg} \right) = 0 \text{ and } \lim_{z \rightarrow 0} \hat{\sigma}_{gg,qg}^{\text{NLO}}(z) = 0$$

- All QCD radiations in the PDF evolution at $\hat{s} \rightarrow \infty$.
- $\hat{\mu}_F$ happens to be a point of minimal scale sensitivity at large \hat{s}

A new scale-choice prescription

JPL, M.A. Ozcelik, EPJC 81 (2021) 6, 497

- The subtraction of the AP CT in the $\overline{\text{MS}}$ -scheme then yields :

$$\lim_{z \rightarrow 0} \hat{\sigma}_{(g,q)g}^{\text{NLO}}(z) = (2C_A, C_F) \frac{\alpha_s}{\pi} \hat{\sigma}_0^{\text{LO}} \left(\log \frac{M_Q^2}{\mu_F^2} + A_{(g,q)g} \right) \quad (3)$$

- In principle, the subtraction should be compensated by the PDF evolution
- PDF evolution is universal, not $A_{ij} \rightarrow \hat{\sigma} < 0$ can arise from this subtraction
- $A_{gg} = A_{qg}$ allows us to propose a new scale prescription for μ_F ,

$$\mu_F = \hat{\mu}_F \equiv M_Q e^{A_{gg,qg}/2} \quad \text{such that } \left(\log \frac{M_Q^2}{\mu_F^2} + A_{gg,qg} \right) = 0 \quad \text{and} \quad \lim_{z \rightarrow 0} \hat{\sigma}_{gg,qg}^{\text{NLO}}(z) = 0$$

- All QCD radiations in the PDF evolution at $\hat{s} \rightarrow \infty$.
- $\hat{\mu}_F$ happens to be a point of minimal scale sensitivity at large \hat{s}
- for η_Q we have $\hat{\mu}_F = \frac{M_Q}{\sqrt{e}} = \begin{cases} 1.82 \text{GeV} & \text{for } \eta_c \text{ with } M_Q = 3 \text{GeV} \\ 5.76 \text{GeV} & \text{for } \eta_b \text{ with } M_Q = 9.5 \text{GeV} \end{cases}$

A new scale-choice prescription

JPL, M.A. Ozcelik, EPJC 81 (2021) 6, 497

- The subtraction of the AP CT in the $\overline{\text{MS}}$ -scheme then yields :

$$\lim_{z \rightarrow 0} \hat{\sigma}_{(g,q)g}^{\text{NLO}}(z) = (2C_A, C_F) \frac{\alpha_s}{\pi} \hat{\sigma}_0^{\text{LO}} \left(\log \frac{M_Q^2}{\mu_F^2} + A_{(g,q)g} \right) \quad (3)$$

- In principle, the subtraction should be compensated by the PDF evolution
- PDF evolution is universal, not $A_{ij} \rightarrow \hat{\sigma} < 0$ can arise from this subtraction
- $A_{gg} = A_{qg}$ allows us to propose a new scale prescription for μ_F ,

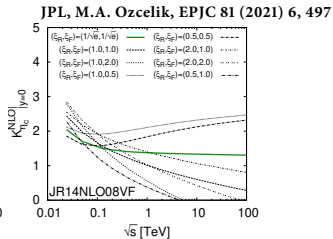
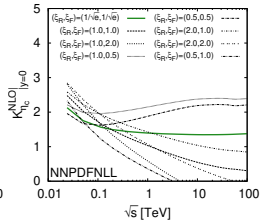
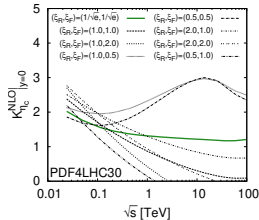
$$\mu_F = \hat{\mu}_F \equiv M_Q e^{A_{gg,qg}/2} \quad \text{such that } \left(\log \frac{M_Q^2}{\mu_F^2} + A_{gg,qg} \right) = 0 \quad \text{and} \quad \lim_{z \rightarrow 0} \hat{\sigma}_{gg,qg}^{\text{NLO}}(z) = 0$$

- All QCD radiations in the PDF evolution at $\hat{s} \rightarrow \infty$.
- $\hat{\mu}_F$ happens to be a point of minimal scale sensitivity at large \hat{s}
- for η_Q we have $\hat{\mu}_F = \frac{M_Q}{\sqrt{e}} = \begin{cases} 1.82 \text{GeV} & \text{for } \eta_c \text{ with } M_Q = 3 \text{GeV} \\ 5.76 \text{GeV} & \text{for } \eta_b \text{ with } M_Q = 9.5 \text{GeV} \end{cases}$
- Such scale choices for η_Q are within usual/conventional bounds $[\frac{M_Q}{2}, 2M_Q]$

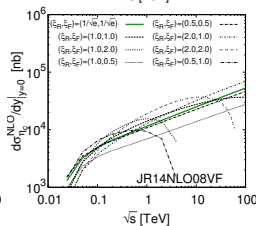
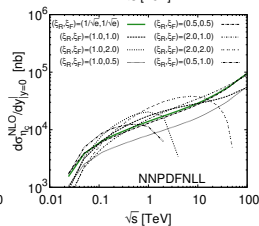
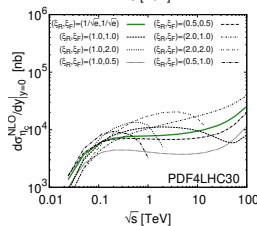
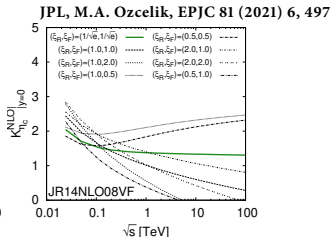
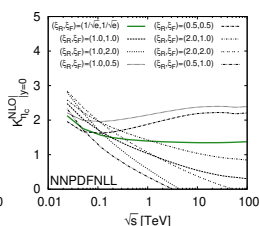
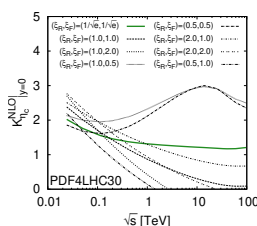
Our results with the $\hat{\mu}_F$ prescription

JPL, M.A. Ozcelik, EPJC 81 (2021) 6, 497

Our results with the $\hat{\mu}_F$ prescription



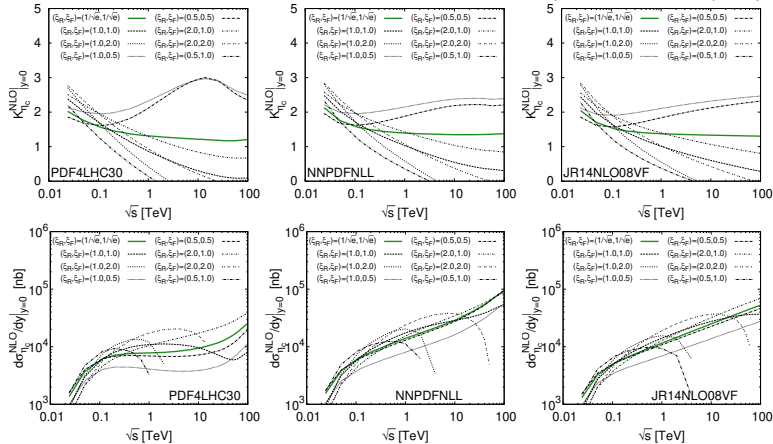
Our results with the $\hat{\mu}_F$ prescription



Problem solved, but it uncovers another: conventional NLO gluon PDFs exhibit a local minimum around $x = 0.001$ at scales below 2 GeV, which distorts $d\sigma(s)/dy$

Our results with the $\hat{\mu}_F$ prescription

JPL, M.A. Ozcelik, EPJC 81 (2021) 6, 497

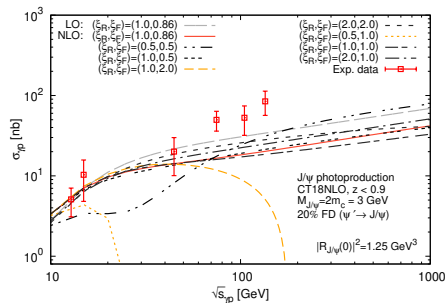


Problem solved, but it uncovers another: conventional NLO gluon PDFs exhibit a local minimum around $x = 0.001$ at scales below 2 GeV, which distorts $d\sigma(s)/dy$

Measuring η_c total cross sections (at NICA, LHC-FT and LHC) : crucial constraints on gluon PDFs

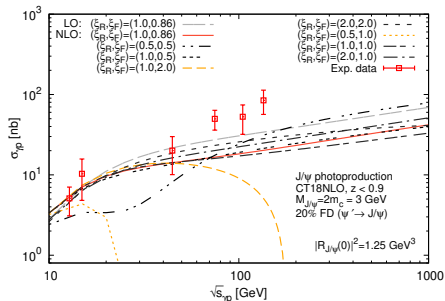
The case of J/ψ photoproduction

A. Colpani Serri, Y. Feng, C. Flore, J.P. Lansberg, M.A. Ozcelik, H.S. Shao, Y. Yedelkina, PLB 835 (2022) 137556



The case of J/ψ photoproduction

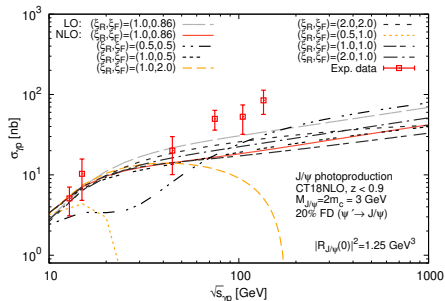
A. Colpani Serri, Y. Feng, C. Flore, J.P. Lansberg, M.A. Ozcelik, H.S. Shao, Y. Yedelkina, PLB 835 (2022) 137556



- NLO cross section for J/ψ photoproduction becomes negative for large μ_F when $\sqrt{s_{J/\psi p}}$ increases

The case of J/ψ photoproduction

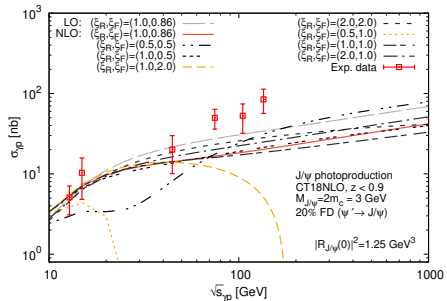
A. Colpani Serri, Y. Feng, C. Flore, J.P. Lansberg, M.A. Ozcelik, H.S. Shao, Y. Yedelkina, PLB 835 (2022) 137556



- NLO cross section for J/ψ photoproduction becomes negative for large μ_F when $\sqrt{s_{\gamma p}}$ increases
- $\hat{s} \rightarrow \infty : \hat{\sigma}_{\gamma i}^{NLO} \propto \alpha_s(\mu_R) \left(\bar{c}_1^{(yi)} \log \frac{M_Q^2}{\mu_F^2} + c_1^{(yi)} \right), A_{\gamma i} = \frac{c_1^{(yi)}}{\bar{c}_1^{(yi)}}, \boxed{A_{\gamma g} = A_{\gamma q}}$

The case of J/ψ photoproduction

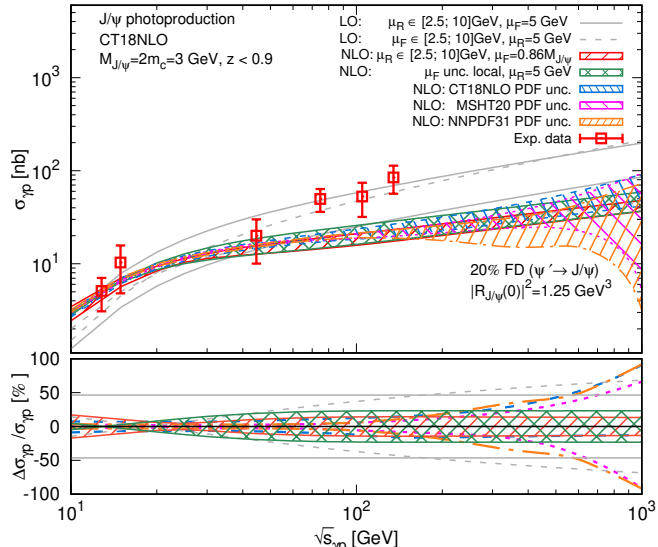
A. Colpani Serri, Y. Feng, C. Flore, J.P. Lansberg, M.A. Ozcelik, H.S. Shao, Y. Yedelkina, PLB 835 (2022) 137556



- NLO cross section for J/ψ photoproduction becomes negative for large μ_F when $\sqrt{s_{\gamma p}}$ increases
 - $\hat{s} \rightarrow \infty : \hat{\sigma}_{\gamma i}^{NLO} \propto \alpha_s(\mu_R) \left(\bar{c}_1^{(\gamma i)} \log \frac{M_Q^2}{\mu_F^2} + c_1^{(\gamma i)} \right), A_{\gamma i} = \frac{c_1^{(\gamma i)}}{\bar{c}_1^{(\gamma i)}}, \boxed{A_{\gamma g} = A_{\gamma q}}$
 - For J/ψ (Υ) photoproduction: $\hat{\mu}_F = 0.86 M_Q$ ($P_T \in [0, \infty], z < 0.9$)

Results with $\hat{\mu}_F = 0.86M_Q$

A. Colpani Serri, Y. Feng, C. Flore, J.P. Lansberg, M.A. Ozcelik, H.S. Shao, Y. Yedelkina PLB 835 (2022) 137556



A word on the P_T -differential cross section

A word on the P_T -differential cross section

- Contrary to a widespread belief, the CSM does a reasonable job in describing the latest large- P_T H1 data

C.Flore, JPL, H.S. Shao, Y. Yedelkina, PLB 811 (2020) 135926

A word on the P_T -differential cross section

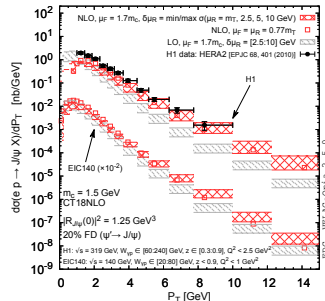
- Contrary to a widespread belief, the CSM does a reasonable job in describing the latest large- P_T H1 data
- The $\hat{\mu}_F$ prescription is not applicable for $d\sigma/dP_T$
- The real-emission contributions ($c_{\gamma i}^{(1)}$) do not scale like born contributions ($\bar{c}_{\gamma i}^{(1)}$)
- $c_{\gamma i}^{(1)}/\bar{c}_{\gamma i}^{(1)} \propto P_T^2$ and this would result in $\hat{\mu}_F(P_T) \propto M_Q e^{P_T/M_Q}$
- $\mu_F = 0.77 m_T$: compromise between $\hat{\mu}_F$ and conventional choices $(0.5; 1; 2)m_T$

C.Flore, JPL, H.S. Shao, Y. Yedelkina, PLB 811 (2020) 135926

A word on the P_T -differential cross section

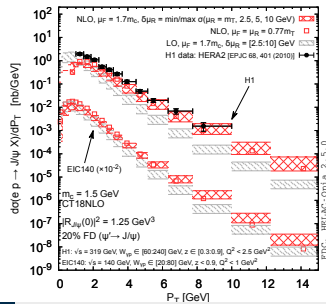
- Contrary to a widespread belief, the CSM does a reasonable job in describing the latest large- P_T H1 data
- The $\hat{\mu}_F$ prescription is not applicable for $d\sigma/dP_T$
- The real-emission contributions ($c_{\gamma i}^{(1)}$) do not scale like born contributions ($\bar{c}_{\gamma i}^{(1)}$)
- $c_{\gamma i}^{(1)}/\bar{c}_{\gamma i}^{(1)} \propto P_T^2$ and this would result in $\hat{\mu}_F(P_T) \propto M_Q e^{P_T/M_Q}$
- $\mu_F = 0.77m_T$: compromise between $\hat{\mu}_F$ and conventional choices $(0.5; 1; 2)m_T$

C.Flore, JPL, H.S. Shao, Y. Yedelkina, PLB 811 (2020) 135926



A word on the P_T -differential cross section

- Contrary to a widespread belief, the CSM does a reasonable job in describing the latest large- P_T H1 data
- The $\hat{\mu}_F$ prescription is not applicable for $d\sigma/dP_T$
- The real-emission contributions ($c_{\gamma i}^{(1)}$) do not scale like born contributions ($\bar{c}_{\gamma i}^{(1)}$)
- $c_{\gamma i}^{(1)}/\bar{c}_{\gamma i}^{(1)} \propto P_T^2$ and this would result in $\hat{\mu}_F(P_T) \propto M_Q e^{P_T/M_Q}$
- $\mu_F = 0.77m_T$: compromise between $\hat{\mu}_F$ and conventional choices (0.5; 1; 2) m_T
- Confirms the good agreement at large P_T and highlights the need for a more systematic solution at low $P_T \rightarrow$ resummation ?



High-energy factorisation: the example of photoproduction

$$\hat{\sigma}_{\text{HEF}}(\eta) \propto \int_0^{1+\eta} \frac{dy}{y} \int_0^{\infty} d\mathbf{q}_{T1}^2 \mathcal{C}\left(\frac{y}{1+\eta}, \mathbf{q}_{T1}^2, \mu_F, \mu_R\right) \mathcal{H}(y, \mathbf{q}_{T1}^2) + \text{NLLA} + O(1/\eta)$$

$$[\eta = (\hat{s} - M_Q^2)/M_Q^2]$$

[Collins, Ellis, 91'; Catani, Ciafaloni, Hautmann, 91'; 94']

High-energy factorisation: the example of photoproduction

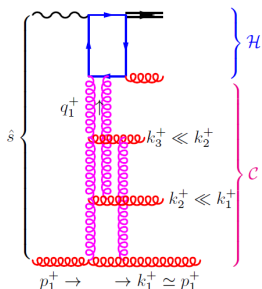
$$\hat{\sigma}_{\text{HEF}}(\eta) \propto \int_0^{1+\eta} \frac{dy}{y} \int_0^\infty d\mathbf{q}_{T1}^2 \mathcal{C}\left(\frac{y}{1+\eta}, \mathbf{q}_{T1}^2, \mu_F, \mu_R\right) \mathcal{H}(y, \mathbf{q}_{T1}^2) + \text{NLLA} + O(1/\eta)$$

$$[\eta = (\hat{s} - M_Q^2)/M_Q^2]$$

[Collins, Ellis, 91'; Catani, Ciafaloni, Hautmann, 91'; 94']

Physical picture in the LLA
for photoproduction:

- LLA: $\sum_n \alpha_s^n \ln^{n-1}(\hat{s}/M_Q^2)$ are resummed



Glauber exchanges ($k_+ k_- \ll \mathbf{k}_T^2$) form the

Reggeised gluon in the t -channel.

High-energy factorisation: the example of photoproduction

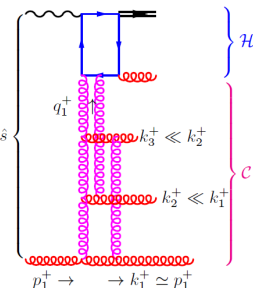
$$\hat{\sigma}_{\text{HEF}}(\eta) \propto \int_0^{1+\eta} \frac{dy}{y} \int_0^\infty d\mathbf{q}_{T1}^2 \mathcal{C}\left(\frac{y}{1+\eta}, \mathbf{q}_{T1}^2, \mu_F, \mu_R\right) \mathcal{H}(y, \mathbf{q}_{T1}^2) + \text{NLLA} + O(1/\eta)$$

$$[\eta = (\hat{s} - M_Q^2)/M_Q^2]$$

[Collins, Ellis, 91'; Catani, Ciafaloni, Hautmann, 91'; 94']

Physical picture in the LLA
for photoproduction:

- LLA: $\sum_n \alpha_s^n \ln^{n-1}(\hat{s}/M_Q^2)$ are resummed
- \mathcal{H} known at LO in α_s (sufficient for LLA)



$RR \rightarrow Q X$: Hagler et.al PRL 86 (2001) 1446; Kniehl, Vasin, Saleev PRD 73 (2006) 074022

$yR \rightarrow Q X$: Baranov, Lipatov, Zotov, EPJC 71 (2011) 1631; KVS, PRD 73 (2006) 074022

Glauber exchanges ($k_+ k_- \ll \mathbf{k}_T^2$) form the

Reggeised gluon in the t -channel.

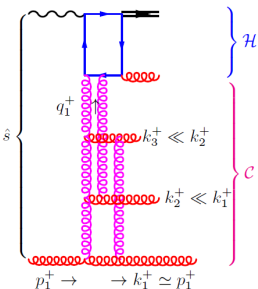
High-energy factorisation: the example of photoproduction

$$\hat{\sigma}_{\text{HEF}}(\eta) \propto \int_0^{1+\eta} \frac{dy}{y} \int_0^\infty d\mathbf{q}_{T1}^2 \mathcal{C}\left(\frac{y}{1+\eta}, \mathbf{q}_{T1}^2, \mu_F, \mu_R\right) \mathcal{H}(y, \mathbf{q}_{T1}^2) + \text{NLLA} + O(1/\eta)$$

$$[\eta = (\hat{s} - M_Q^2)/M_Q^2]$$

[Collins, Ellis, 91'; Catani, Ciafaloni, Hautmann, 91'; 94']

Physical picture in the LLA
for photoproduction:



Glauber exchanges ($k_+ k_- \ll \mathbf{k}_T^2$) form the

Reggeised gluon in the t -channel.

- LLA: $\sum_n \alpha_s^n \ln^{n-1}(\hat{s}/M_Q^2)$ are resummed

- \mathcal{H} known at LO in α_s (sufficient for LLA)

$RR \rightarrow Q X$: Hagler et.al PRL 86 (2001) 1446; Kniehl, Vasin, Saleev PRD 73 (2006) 074022

$yR \rightarrow Q X$: Baranov, Lipatov, Zotov, EPJC 71 (2011) 1631; KVS, PRD 73 (2006) 074022

- The resummation factors \mathcal{C} are the solution of the LL BFKL with the collinear divergences subtracted

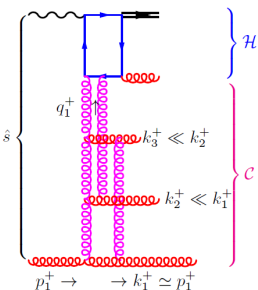
High-energy factorisation: the example of photoproduction

$$\hat{\sigma}_{\text{HEF}}(\eta) \propto \int_0^{1+\eta} \frac{dy}{y} \int_0^\infty d\mathbf{q}_{T1}^2 \mathcal{C}\left(\frac{y}{1+\eta}, \mathbf{q}_{T1}^2, \mu_F, \mu_R\right) \mathcal{H}(y, \mathbf{q}_{T1}^2) + \text{NLLA} + O(1/\eta)$$

$$[\eta = (\hat{s} - M_Q^2)/M_Q^2]$$

[Collins, Ellis, 91'; Catani, Ciafaloni, Hautmann, 91'; 94']

Physical picture in the LLA
for photoproduction:



Glauber exchanges ($k_+ k_- \ll \mathbf{k}_T^2$) form the

Reggeised gluon in the t -channel.

- LLA: $\sum_n \alpha_s^n \ln^{n-1}(\hat{s}/M_Q^2)$ are resummed

- \mathcal{H} known at LO in α_s (sufficient for LLA)

$RR \rightarrow QX$: Hagler et.al PRL 86 (2001) 1446; Kniehl, Vasin, Saleev PRD 73 (2006) 074022

$yR \rightarrow QX$: Baranov, Lipatov, Zotov, EPJC 71 (2011) 1631; KVS, PRD 73 (2006) 074022

- The resummation factors \mathcal{C} are the solution of the LL BFKL with the collinear divergences subtracted
- The expansion in α_s of $\hat{\sigma}_{\text{HEF}}(\hat{s})$ **should coincide** with $\hat{\sigma}_{\text{NLO}}(\hat{s} \rightarrow \infty)$ and predicts $\hat{\sigma}_{\text{NNLO}}(\hat{s} \rightarrow \infty)$

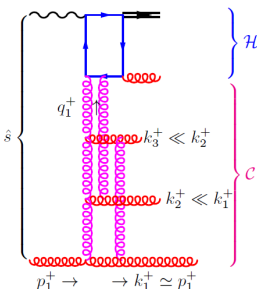
High-energy factorisation: the example of photoproduction

$$\hat{\sigma}_{\text{HEF}}(\eta) \propto \int_0^{1+\eta} \frac{dy}{y} \int_0^\infty d\mathbf{q}_{T1}^2 \mathcal{C}\left(\frac{y}{1+\eta}, \mathbf{q}_{T1}^2, \mu_F, \mu_R\right) \mathcal{H}(y, \mathbf{q}_{T1}^2) + \text{NLLA} + O(1/\eta)$$

$$[\eta = (\hat{s} - M_Q^2)/M_Q^2]$$

[Collins, Ellis, 91'; Catani, Ciafaloni, Hautmann, 91'; 94']

Physical picture in the LLA
for photoproduction:



Glauber exchanges ($k_+ k_- \ll \mathbf{k}_T^2$) form the

Reggeised gluon in the t -channel.

- LLA: $\sum_n \alpha_s^n \ln^{n-1}(\hat{s}/M_Q^2)$ are resummed

- \mathcal{H} known at LO in α_s (sufficient for LLA)

$RR \rightarrow QX$: Hagler et.al PRL 86 (2001) 1446; Kniehl, Vasin, Saleev PRD 73 (2006) 074022

$yR \rightarrow QX$: Baranov, Lipatov, Zotov, EPJC 71 (2011) 1631; KVS, PRD 73 (2006) 074022

- The resummation factors \mathcal{C} are the solution of the LL BFKL with the collinear divergences subtracted
- The expansion in α_s of $\hat{\sigma}_{\text{HEF}}(\hat{s})$ **should coincide** with $\hat{\sigma}_{\text{NLO}}(\hat{s} \rightarrow \infty)$ and predicts $\hat{\sigma}_{\text{NNLO}}(\hat{s} \rightarrow \infty)$
- HEF can be used with the same collinear PDFs as CF and can be matched on to CF [better to use DLA for consistency]

Consistency check for $pp \rightarrow QX$

J.P. Lansberg, M. Nefedov, M.A.Ozcelik, JHEP 05 (2022) 083

HEF expanded up to NLO in α_s should reproduce the $A_1^{[m]}$ NLO coefficient

Consistency check for $pp \rightarrow QX$

J.P. Lansberg, M. Nefedov, M.A.Ozcelik, JHEP 05 (2022) 083

HEF expanded up to NLO in α_s should reproduce the $A_1^{[m]}$ NLO coefficient

High-energy limit (for $pp \rightarrow QX$ with $z = \frac{M_Q^2}{\hat{s}}$):

$$\hat{\sigma}_{gg}^{[m], \text{HEF}}(z \rightarrow 0) = \sigma_{\text{LO}}^{[m]} \left\{ A_0^{[m]} \delta(1-z) + \frac{\alpha_s}{\pi} 2C_A \left[A_1^{[m]} + A_0^{[m]} \ln \frac{M^2}{\mu_F^2} \right] + \left(\frac{\alpha_s}{\pi} \right)^2 \ln \frac{1}{z} C_A^2 \left[2A_2^{[m]} + B_2^{[m]} + 4A_1^{[m]} \ln \frac{M^2}{\mu_F^2} + 2A_0^{[m]} \ln^2 \frac{M^2}{\mu_F^2} \right] + O(\alpha_s^3) \right\},$$

Consistency check for $pp \rightarrow QX$

J.P. Lansberg, M. Nefedov, M.A.Ozcelik, JHEP 05 (2022) 083

HEF expanded up to NLO in α_s should reproduce the $A_1^{[m]}$ NLO coefficient

High-energy limit (for $pp \rightarrow QX$ with $z = \frac{M_Q^2}{\hat{s}}$):

$$\hat{\sigma}_{gg}^{[m], \text{HEF}}(z \rightarrow 0) = \sigma_{\text{LO}}^{[m]} \left\{ A_0^{[m]} \delta(1-z) + \frac{\alpha_s}{\pi} 2C_A \left[A_1^{[m]} + A_0^{[m]} \ln \frac{M^2}{\mu_F^2} \right] + \left(\frac{\alpha_s}{\pi} \right)^2 \ln \frac{1}{z} C_A^2 \left[2A_2^{[m]} + B_2^{[m]} + 4A_1^{[m]} \ln \frac{M^2}{\mu_F^2} + 2A_0^{[m]} \ln^2 \frac{M^2}{\mu_F^2} \right] + O(\alpha_s^3) \right\},$$

From HEF, up to NNLO in α_s , one has

State	$A_0^{[m]}$	$A_1^{[m]}$	$A_2^{[m]}$	$B_2^{[m]}$
1S_0	1	-1	$\frac{\pi^2}{6}$	$\frac{\pi^2}{6}$
3S_1	0	1	0	$\frac{\pi^2}{6}$
3P_0	1	$-\frac{43}{27}$	$\frac{\pi^2}{6} + \frac{2}{3}$	$\frac{\pi^2}{6} + \frac{40}{27}$
3P_1	0	$\frac{5}{54}$	$-\frac{1}{9}$	$-\frac{2}{9}$
3P_2	1	$-\frac{53}{36}$	$\frac{\pi^2}{6} + \frac{1}{2}$	$\frac{\pi^2}{6} + \frac{11}{9}$

Consistency check for $pp \rightarrow QX$

J.P. Lansberg, M. Nefedov, M.A.Ozcelik, JHEP 05 (2022) 083

HEF expanded up to NLO in α_s should reproduce the $A_1^{[m]}$ NLO coefficient

High-energy limit (for $pp \rightarrow QX$ with $z = \frac{M_Q^2}{\hat{s}}$):

$$\hat{\sigma}_{gg}^{[m], \text{HEF}}(z \rightarrow 0) = \sigma_{\text{LO}}^{[m]} \left\{ A_0^{[m]} \delta(1-z) + \frac{\alpha_s}{\pi} 2C_A \left[A_1^{[m]} + A_0^{[m]} \ln \frac{M^2}{\mu_F^2} \right] + \left(\frac{\alpha_s}{\pi} \right)^2 \ln \frac{1}{z} C_A^2 \left[2A_2^{[m]} + B_2^{[m]} + 4A_1^{[m]} \ln \frac{M^2}{\mu_F^2} + 2A_0^{[m]} \ln^2 \frac{M^2}{\mu_F^2} \right] + O(\alpha_s^3) \right\},$$

From HEF, up to NNLO in α_s , one has

State	$A_0^{[m]}$	$A_1^{[m]}$	$A_2^{[m]}$	$B_2^{[m]}$
1S_0	1	-1	$\frac{\pi^2}{6}$	$\frac{\pi^2}{6}$
3S_1	0	1	0	$\frac{\pi^2}{6}$
3P_0	1	$-\frac{43}{27}$	$\frac{\pi^2}{6} + \frac{2}{3}$	$\frac{\pi^2}{6} + \frac{40}{27}$
3P_1	0	$\frac{5}{54}$	$-\frac{1}{9}$	$-\frac{2}{9}$
3P_2	1	$-\frac{53}{36}$	$\frac{\pi^2}{6} + \frac{1}{2}$	$\frac{\pi^2}{6} + \frac{11}{9}$

Perfect match for NLO and prediction for NNLO !

NLO: JPL, M.A. Ozcelik, EPJC 81 (2021) 6, 497

Matching HEF and NLO CF (illustration for η_Q)

The HEF works only at $z \ll 1$ and does not include corrections $O(z)$, while NLO CF is exact in z but only NLO up to α_s . **We need to match them.**

Matching HEF and NLO CF (illustration for η_Q)

The HEF works only at $z \ll 1$ and does not include corrections $O(z)$, while NLO CF is exact in z but only NLO up to α_s . **We need to match them.**

- Simplest prescription: just **subtract the overlap** at $z \ll 1$ where $\text{CF} \subset \text{HEF}$:

$$\sigma_{\text{NLO+HEF}}^{[m]} = \sigma_{\text{LO CF}}^{[m]} + \int_{z_{\min}}^1 \frac{dz}{z} \left[\check{\sigma}_{\text{HEF}}^{[m],ij}(z) + \hat{\sigma}_{\text{NLO CF}}^{[m],ij}(z) - \hat{\sigma}_{\text{NLO CF}}^{[m],ij}(0) \right] \mathcal{L}_{ij}(z)$$

Matching HEF and NLO CF (illustration for η_Q)

The HEF works only at $z \ll 1$ and does not include corrections $O(z)$, while NLO CF is exact in z but only NLO up to α_s . **We need to match them.**

- Simplest prescription: just **subtract the overlap** at $z \ll 1$ where $\text{CF} \subset \text{HEF}$:

$$\sigma_{\text{NLO+HEF}}^{[m]} = \sigma_{\text{LO CF}}^{[m]} + \int_{z_{\min}}^1 \frac{dz}{z} \left[\check{\sigma}_{\text{HEF}}^{[m],ij}(z) + \hat{\sigma}_{\text{NLO CF}}^{[m],ij}(z) - \hat{\sigma}_{\text{NLO CF}}^{[m],ij}(0) \right] \mathcal{L}_{ij}(z)$$

- Or introduce **smooth weights**:

$$\begin{aligned} \sigma_{\text{NLO+HEF}}^{[m]} = & \sigma_{\text{LO CF}}^{[m]} + \int_{z_{\min}}^1 dz \left\{ \left[\check{\sigma}_{\text{HEF}}^{[m],ij}(z) \frac{\mathcal{L}_{ij}(z)}{z} \right] w_{\text{HEF}}^{ij}(z) \right. \\ & \left. + \left[\hat{\sigma}_{\text{NLO CF}}^{[m],ij}(z) \frac{\mathcal{L}_{ij}(z)}{z} \right] (1 - w_{\text{HEF}}^{ij}(z)) \right\}, \end{aligned}$$

Inverse-error-weighting method

M.G. Echevarria, T. Kasemets, JPL, C. Pisano, A. Signori, PLB 781 (2018) 161

In the InEW method, the weights are calculated from the **parametric estimates of the error** of each contribution and combined as such:

$$w_{\text{HEF}}^{ij}(z) = \frac{[\Delta\sigma_{\text{HEF}}^{ij}(z)]^{-2}}{[\Delta\sigma_{\text{HEF}}^{ij}(z)]^{-2} + [\Delta\sigma_{\text{CF}}^{ij}(z)]^{-2}},$$

Inverse-error-weighting method

M.G. Echevarria, T. Kasemets, JPL, C. Pisano, A. Signori, PLB 781 (2018) 161

In the InEW method, the weights are calculated from the **parametric estimates of the error** of each contribution and combined as such:

$$w_{\text{HEF}}^{ij}(z) = \frac{[\Delta\sigma_{\text{HEF}}^{ij}(z)]^{-2}}{[\Delta\sigma_{\text{HEF}}^{ij}(z)]^{-2} + [\Delta\sigma_{\text{CF}}^{ij}(z)]^{-2}},$$

$\sigma_{\text{CF}}^{\text{NLO}}$ misses HO terms in α_s . Our $\Delta\sigma_{\text{CF}}$ includes estimates of NNLO $\alpha_s^2 \ln \frac{\hat{s}}{M_Q^2}$ terms of $\hat{\sigma}_{\text{HEF}}$ + a generic NNLO uncertainty $\alpha_s^2 \mathcal{O}(1) \rightarrow \alpha_s \hat{\sigma}_{\text{CF}}^{\text{NLO}}$

Inverse-error-weighting method

M.G. Echevarria, T. Kasemets, JPL, C. Pisano, A. Signori, PLB 781 (2018) 161

In the InEW method, the weights are calculated from the **parametric estimates of the error** of each contribution and combined as such:

$$w_{\text{HEF}}^{ij}(z) = \frac{[\Delta\sigma_{\text{HEF}}^{ij}(z)]^{-2}}{[\Delta\sigma_{\text{HEF}}^{ij}(z)]^{-2} + [\Delta\sigma_{\text{CF}}^{ij}(z)]^{-2}},$$

$\hat{\sigma}_{\text{CF}}^{\text{NLO}}$ misses HO terms in α_s . Our $\Delta\sigma_{\text{CF}}$ includes estimates of NNLO $\alpha_s^2 \ln \frac{\hat{s}}{M_Q^2}$ terms of $\hat{\sigma}_{\text{HEF}}$ + a generic NNLO uncertainty $\alpha_s^2 \mathcal{O}(1) \rightarrow \alpha_s \hat{\sigma}_{\text{CF}}^{\text{NLO}}$

$\hat{\sigma}_{\text{HEF}}^{\text{LLA}}$ misses HO terms in $\frac{M_Q^2}{\hat{s}}$. Our $\Delta\sigma_{\text{HEF}}$ includes estimates of NLLA corrections as $\alpha_s^2 \mathcal{O}\left(\frac{M_Q^2}{\hat{s}}\right) \rightarrow \alpha_s \hat{\sigma}_{\text{CF}}^{\text{NLO}} + \left(\frac{M_Q^2}{\hat{s}}\right)^\alpha (\hat{\sigma}_{\text{CF}}^{\text{NLO}}(\hat{s}) - \hat{\sigma}_{\text{CF}}^{\text{NLO}}(\infty))$ term

Inverse-error-weighting method

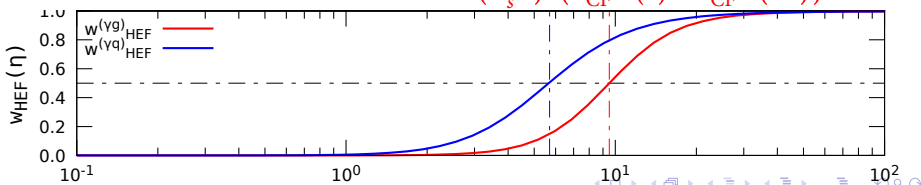
M.G. Echevarria, T. Kasemets, JPL, C. Pisano, A. Signori, PLB 781 (2018) 161

In the InEW method, the weights are calculated from the **parametric estimates of the error** of each contribution and combined as such:

$$w_{\text{HEF}}^{ij}(z) = \frac{[\Delta\sigma_{\text{HEF}}^{ij}(z)]^{-2}}{[\Delta\sigma_{\text{HEF}}^{ij}(z)]^{-2} + [\Delta\sigma_{\text{CF}}^{ij}(z)]^{-2}},$$

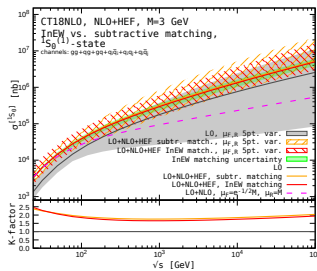
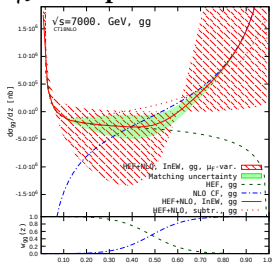
$\hat{\sigma}_{\text{CF}}^{\text{NLO}}$ misses HO terms in α_s . Our $\Delta\sigma_{\text{CF}}$ includes estimates of NNLO $\alpha_s^2 \ln \frac{\hat{s}}{M_Q^2}$ terms of $\hat{\sigma}_{\text{HEF}}$ + a generic NNLO uncertainty $\alpha_s^2 \mathcal{O}(1) \rightarrow \alpha_s \hat{\sigma}_{\text{CF}}^{\text{NLO}}$

$\sigma_{\text{HEF}}^{\text{LLA}}$ misses HO terms in $\frac{M_Q^2}{\hat{s}}$. Our $\Delta\sigma_{\text{HEF}}$ includes estimates of NLLA corrections as $\alpha_s^2 \mathcal{O}\left(\frac{M_Q^2}{\hat{s}}\right) \rightarrow \alpha_s \hat{\sigma}_{\text{CF}}^{\text{NLO}} + \left(\frac{M_Q^2}{\hat{s}}\right)^\alpha (\hat{\sigma}_{\text{CF}}^{\text{NLO}}(\hat{s}) - \hat{\sigma}_{\text{CF}}^{\text{NLO}}(\infty))$ term



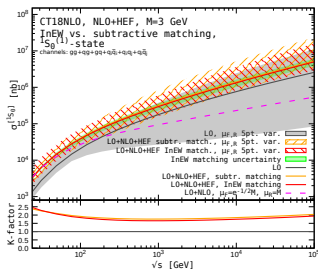
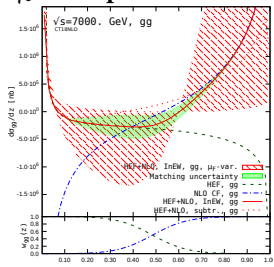
Matched results η_c hadroproduction

JPL, M. Nefedov, M.A.Ozcelik, JHEP 05 (2022) 083 and 2306.02425(to appear in EPJC)

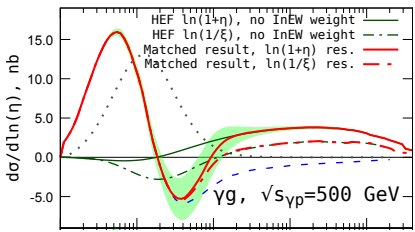


Matched results η_c hadroproduction

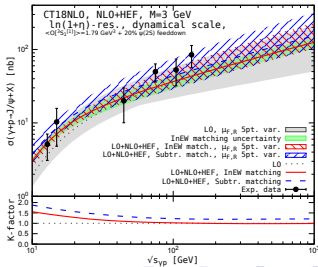
JPL, M. Nefedov, M.A.Ozcelik, JHEP 05 (2022) 083 and 2306.02425(to appear in EPJC)



J/ψ photoproduction

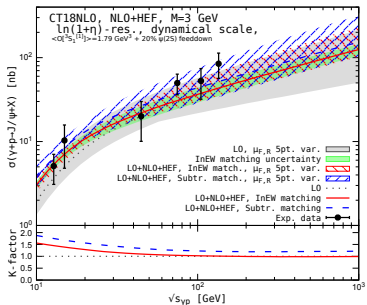


For this plot: dashed blue: CF NLO



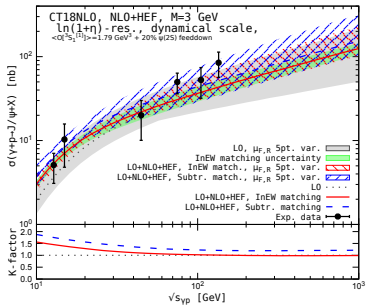
Discussion

JPL, M. Nefedov, M.A.Ozcelik 2306.02425(to appear in EPJC)



Discussion

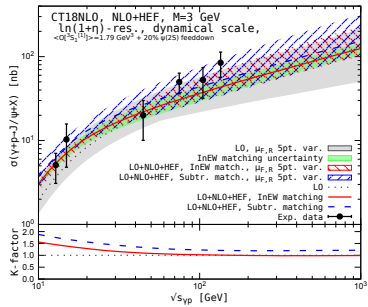
JPL, M. Nefedov, M.A.Ozcelik 2306.02425(to appear in EPJC)



- NLO matched results now show a **sane energy dependence**;

Discussion

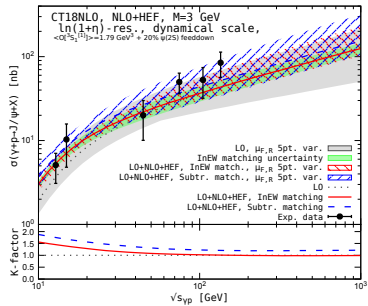
JPL, M. Nefedov, M.A.Ozcelik 2306.02425(to appear in EPJC)



- NLO matched results now show a **sane energy dependence**;
- Good **agreement** with **data**;

Discussion

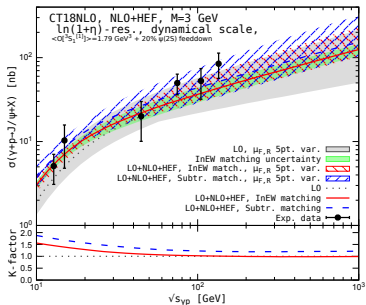
JPL, M. Nefedov, M.A.Ozcelik 2306.02425(to appear in EPJC)



- NLO matched results now show a **sane energy dependence**;
- Good **agreement** with **data**;
- The **scale uncertainties** at NLO are smaller than at LO;

Discussion

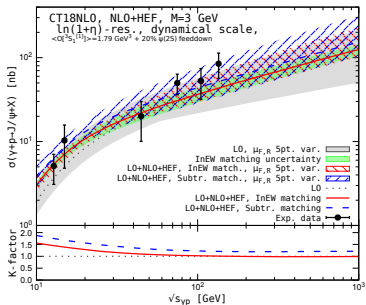
JPL, M. Nefedov, M.A.Ozcelik 2306.02425(to appear in EPJC)



- NLO matched results now show a **sane energy dependence**;
- Good **agreement** with **data**;
- The **scale uncertainties** at NLO are smaller than at LO;
- InEW and subtractive matchings give similar results, their difference is compatible with the **InEW matching uncertainty**;

Discussion

JPL, M. Nefedov, M.A.Ozcelik 2306.02425(to appear in EPJC)



- NLO matched results now show a **sane energy dependence**;
- Good **agreement** with **data**;
- The **scale uncertainties** at NLO are smaller than at LO;
- InEW and subtractive matchings give similar results, their difference is compatible with the **InEW matching uncertainty**;
- Further reduction of the theory uncertainty calls for a **NLLA** computation;

Outlook I

Outlook I

- Apply HEF @ LLA to $pp \rightarrow \chi_c X$ (worst case) and to $pp \rightarrow \psi X$

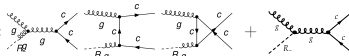
Outlook I

- Apply HEF @ LLA to $pp \rightarrow \chi_c X$ (worst case) and to $pp \rightarrow \psi X$
- Progress towards the first NLLA computation for quarkonia

M. Nefedov 2309.09608

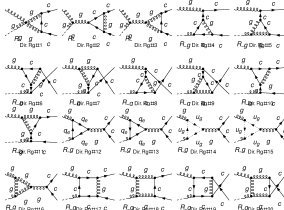
$Rg \rightarrow c\bar{c} [{}^1S_0^{[1]}]$ and $c\bar{c} [{}^3S_1^{[8]}]$ @ 1 loop

Interference with LO:



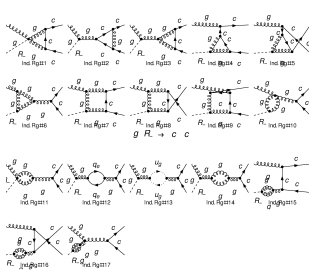
Induced Rgg coupling diagrams:

Some Rg -coupling diagrams:



and so on...

$g Rg \rightarrow c c$

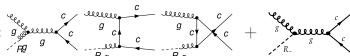


Outlook I

- Apply HEF @ LLA to $pp \rightarrow \chi_c X$ (worst case) and to $pp \rightarrow \psi X$
- Progress towards the **first NLLA computation** for quarkonia M. Nefedov 2309.09608
→ **Virtual corr. done**, with the expected IR and rapidity divergence structure

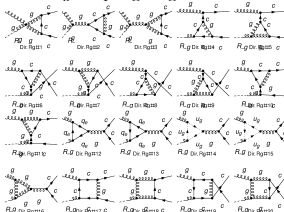
$Rg \rightarrow c\bar{c} \left[{}^1S_0^{[1]}\right]$ and $c\bar{c} \left[{}^3S_1^{[8]}\right]$ @ 1 loop

Interference with LO:



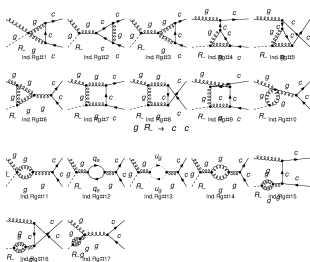
Induced Rgg coupling diagrams:

Some Rg -coupling diagrams:



and so on...

$g Rg \rightarrow c c$



Outlook II

Progress in Particle and Nuclear Physics 122 (2021) 103986

Contents lists available at ScienceDirect

Progress in Particle and Nuclear Physics

ELSEVIER

journal homepage: www.elsevier.com/locate/ppnp



Review

Prospects for quarkonium studies at the high-luminosity LHC

Émilien Chapon^{1,2}, David d'Enterria^{3,4}, Bertrand Ducloué^{5,6}, Miguel Echevarria^{3,6}, Pol-Bernard Gossiaux^{3,6}, Vato Kartvelishvili^{3,6}, Tomas Kasemets^{7,8}, Jean-Philippe Lansberg^{3,6,9}, Ronan McNulty^{3,6}, Darren D. Price^{10,11}, Hua-Sheng Shao^{11,12}, Charlotte Van Hulse^{3,6}, Michael Winn^{12,13}, Jaroslav Adam¹², Liupan An¹³, Denys Yen Arrebato Villar³, Shohini Bhattacharya¹³, Francesco G. Celiberto^{16,17,18,19}, Cvetan Cheshkov²⁰, Umberto D'Alesio²¹, Cesar da Silva²², Elena G. Ferreiro²³, Chris A. Flett^{24,25}, Carlo Flory³, Maria Vittoria Garzelli^{26,27,28}, Jonathan Gaunt^{28,29}, Jibo He²⁹, Yiannis Makris¹², Cyrille Marquet³⁰, Laure Massacrier³¹, Thomas Mehen³¹, Cédric Mezrag¹², Luca Micheletti²², Riccardo Nagar¹², Maxim A. Nefedov³², Melih A. Ozcelik³³, Biswarup Paul²¹, Cristian Pisano¹², Jian-Wei Qiu³⁵, Sangem Rajesh²¹, Matteo Rinaldi³⁶, Florent Scarpa^{30,37}, Maddie Smith³⁸, Pieter Taels³⁹, Amy Tee³⁹, Oleg Teryaev³⁸, Ivan Vitev²², Kazuhiro Watanabe³⁵, Nodoka Yamanaka^{29,30}, Xiaojun Yao⁴¹, Yanxi Zhang³².



1. Introduction

2. Proton-proton collisions

3. Exclusive and diffractive production

4. Transverse-Momentum-Dependent effects in inclusive reactions

5. Proton-nucleus collisions

6. Nucleus-nucleus collisions

7. Double and triple parton scatterings

8. Summary

Physics case for quarkonium studies at the Electron Ion Collider

Editors: Daniel Boer^{a,1}, Carlo Flory^{b,1}, Daniel Kikola^{c,1}, Jean-Philippe Lansberg^{b,1}, Charlotte Van Hulse^{b,1}

^aVan Swinderen Institute for Particle Physics and Gravity, University of Groningen, 9747 AG Groningen, The Netherlands

^bUniversité Paris-Saclay, CNRS/IN2P3, IJCLab, 91405 Orsay, France

^cFaculty of Physics, Warsaw University of Technology, ul. Koszykowa 75, 00-662 Warsaw, Poland

Abstract

The physics case for quarkonium-production studies accessible at the future US Electron Ion Collider is described.

1. Introduction

2. Generalities about quarkonium studies at the EIC

3. EIC tools for quarkonium studies

4. Quarkonia as tools to study the parton content of the nucleons

5. Quarkonia as tools to study the parton content of the nuclei

6. Summary

A EU Virtual Access to pQCD tools: NLOAccess

[in2p3.fr/nloaccess]

The screenshot shows the homepage of the NLOAccess project. At the top, there's a banner with the text "Virtual Access: Automated perturbative NLO calculations for heavy ions and quarkonia (NLOAccess)" and a background image of a wooden surface with a coffee cup. Below the banner, the word "NLOAccess" is prominently displayed in large white letters on an orange background. The main content area has a light blue header with the title "GENERAL DESCRIPTION". Under this, there's a section titled "Objectives:" followed by a detailed paragraph about the project's purpose. A "Show more" link is present at the end of this section. To the right, there's a "FOLLOW:" section featuring the "STRONG 2020" logo, which includes the European Union flag. Below the logo, there's a block of text about funding from the European Union's Horizon 2020 research and innovation programme.

NLOAccess

Virtual Access: Automated perturbative NLO calculations for heavy ions and quarkonia (NLOAccess)

Home The project News Tools Request registration

GENERAL DESCRIPTION

Objectives:

NLOAccess will give access to automated tools generating scientific codes allowing anyone to evaluate observables -such as production rates or kinematical properties – of scatterings involving hadrons. The automation and the versatility of these tools are such that these scatterings need not to be pre-coded. In other terms, it is possible that a random user may request for the first time the generation of a code to compute characteristics of a reaction which nobody thought of before. NLOAccess will allow the user to test the code and then to download to run it on its own computer. It essentially gives access to a dynamical library

[Show more](#)

FOLLOW:

STRONG 2020

This project has received funding from the European Union's Horizon 2020 research and innovation programme under grant agreement No. 824093.

HELAC-Onia Web [nloaccess.in2p3.fr/HO/]

HELAC-Onia Web

[Request Registration](#)

[References](#)

[Contact us](#)

[Login](#)



Automated perturbative calculation with HELAC-Onia Web

Welcome to HELAC-Onia Web!

HELAC-Onia is an automatic matrix element generator for the calculation of the heavy quarkonium helicity amplitudes in the framework of NRQCD factorization.

The program is able to calculate helicity amplitudes of multi P-wave quarkonium states production at hadron colliders and electron-positron colliders by including new P-wave off-shell currents. Besides the high efficiencies in computation of multi-leg processes within the Standard Model, HELAC-Onia is also sufficiently numerical stable in dealing with P-wave quarkonia and P-wave color-octet intermediate states.

Already registered to the portal? Please [login](#).

Do you not have an account? Make a [registration request](#).



MG5@NLO online [nloaccess.in2p3.fr/MG5/]

 MG5_aMC@NLO

[Request Registration](#)

[References](#)

 [Contact us](#)

 [Login](#)



Automated perturbative calculation with NLOAccess

MG5_aMC@NLO

MadGraph5_aMC@NLO is a framework that aims at providing all the elements necessary for SM and BSM phenomenology, such as the computations of cross sections, the generation of hard events and their matching with event generators, and the use of a variety of tools relevant to event manipulation and analysis. Processes can be simulated to LO accuracy for any user-defined Lagrangian, an the NLO accuracy in the case of models that support this kind of calculations -- prominent among these are QCD and EW corrections to SM processes. Matrix elements at the tree- and one-loop-level can also be obtained.

Please login to use MG5_aMC@NLO.

